

Development and property study of the extremely thin 12 μm -type straw tubes with 5-mm diameter for a Straw Tracker System of COMET

N. Tsverava^{a,b,*}, G. Adamov^{a,d}, D. Chokheli^{a,b}, H. Nishiguchi^c,
T. Toriashvili^a, Z. Tsamalaidze^{a,b}

^aGeorgian Technical University, Tbilisi, Georgia

^bJoint Institute for Nuclear Research, Dubna, Russia

^cHigh Energy Accelerator Research Organization (KEK), Tsukuba, Japan

^dGraduate University for Advanced Studies (SOKENDAI), Tsukuba, Japan

Abstract

The COMET experiment focuses on searching for the direct conversion of a muon into an electron with aluminum nuclei without emitting a neutrino (so-called $\mu \rightarrow e$ conversion). This conversion violates charged lepton flavor conservation law, a fundamental principle in the Standard Model. The COMET experiment requirement is to achieve the muon-to-electron conversion sensitivity on a level of 10^{-17} . The Straw Tracker System (STS) based on straw tubes could provide the necessary spatial resolution of 150 μm and the electron momentum resolution better than 200 keV/c.

The COMET experiment will be separated into two phases. Phase-I will operate with the 3.2 kW 8-GeV-proton beam, and Phase-II will operate with beam intensity increased to 56 kW. STS must operate in a vacuum with 1 bar internal pressure applied to straws. The initial design of 10-mm-diameter straws developed for phase-I will not be as efficient with the 20 times increased beam intensity of Phase II, but the new STS design based on 5-mm-diameter 12- μm thick straws could fully satisfy the required efficiency. The mechanical properties of these straws, such as sagging, elongation, dependence of the diameter on over-pressure, etc, are discussed in this article.

Keywords: The COMET Straw Tracker System, COMET STS, 5-mm-diameter straw tube, straw tubes mechanical properties, ultrasonic welding technologies

*Corresponding author

Email address: Nikoloz.Tsverava@cern.ch (N. Tsverava)

1. Introduction

The COMET (COherent Muon to Electron Transition) experiment [1] is aiming to search for neutrinoless muon-to-electron conversion. This process lies beyond the Standard Model (SM) [2-5]. The straw tracker system (STS) is an essential part of the COMET experiment. The main advantage of straw chambers is reduced multiple scattering due to very low material with low density on the charged particle's propagation path, which increases the energy resolution for this particle, holding the momentum resolution better than 2% for 100 MeV region. This allows us to achieve a single-event sensitivity below 10^{-16} [6].

Historically, the straw tube system was first proposed as a tracking system for the Superconducting Super Collider (SSC, [7, 8]) in 1989. And the trackers based on it were introduced for COMPASS experiment [9] and were widely in use at experiments such as PANDA [10], ATLAS[11], etc. The straw for these experiments was done by S-cladding technology when thin ($36\ \mu\text{m}$) a mylar film with Al or other metal layer deposit on it is winded around an axis with steps in between, thus creating the tubing. For instance, the straws for Straw-tube Tracker, for Mu2e experiment [12] were made with such technology.

The other type, C-type cladding technology, of the straw production was introduced for NA62 Low Mass Straw Tracker [13] when the 10-mm-diameter tube shape was formed from flat mylar film with $36\ \mu\text{m}$ in thickness and a seam was welded with ultrasonic welder thus creating the tubing. Straws with such technology will also be used for COMET Straw Tracker [14]. The straws for COMET Phase-I are 10 mm in diameter, and mylar thickness is $20\ \mu\text{m}$.

But COMET phase-II proposed operating with the 8 GeV proton beam upgraded from 3.2 kW for COMET Phase-I to 56 kW for Phase-II [15]. It increases the muon beam from $5 \times 10^9\ \mu/s$ for COMET Phase-I to $1 \times 10^{11}\ \mu/s$ for COMET Phase-II. With these new conditions, the COMET STS should be improved to hold the spatial and momentum resolution requirements at the same level but at an increased rate. The new design of the STS was proposed ([16]) based on 5-mm diameter straw tubes created using thinner - $12\ \mu\text{m}$ - mylar to leave the total thickness of the straw system unchanged.

2. The 5 mm 12 μm wall-thick straw tube design and production methods

Two methods can be used to make thin-wall straw tubes, meaning less material for the tracking detector. These are the so-called “doubly wound helix” or S-type straw tubes (Fig. 1a). Another way to create the straw tube is to make the C-shape from the mylar tape by overlapping the edges of the tape and using the ultrasonic welder to stick these edges to each other (“direct adhesion straw” without glue), thus creating the C-type straw (Fig. 1b).

A new method of ultrasonic welding technologies was developed at CERN and adapted by JINR for producing vacuum-compatible C-type straws [17-19]. One of the major advantages of the C-type straw is its low gas leakage rate when operating in a vacuum.

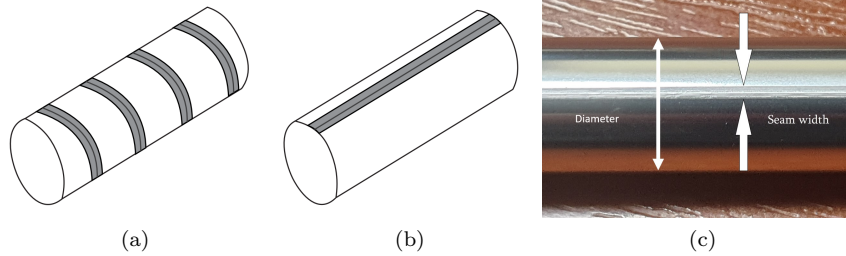


Figure 1: S-type straw tube (a); C-type straw tube with ultrasonic welding (b) and real C-type tube with welding seam (c)

This is the first time the C-type 5-mm-diameter 12- μm straw tube has been produced using the ultrasonic welding technique. So, before creating the whole system with the proposed design, it is necessary to first create the straws according to the required parameters and test their mechanical properties.

2.1. 5-mm-diameter straw tubes design

The main component of the straw tracker for Phase II will be a straw tube with 5 mm diameter [1, 6] and 12- μm thin-walled mylar tube the inner side of which is covered with a 70 nm layer of aluminum (cathode). A gold-plated tungsten wire (anode) is positioned at its center, and high voltage is applied to it. The space between them is filled with $Ar/C2H6(50 : 50)$ mixture working gas under the 1-bar excess pressure. All tracker systems are located inside superconducting magnets with a magnetic field of 1 Tesla and operate in a vacuum.

2.2. Ultrasonic welding production station

The C-type straw tube production station based on ultrasonic welding technology was built from scratch, focusing on 5-mm diameter 12 μm wall-thick 2-m-long straw production. For a welding process, an ultrasonic generator with 44 kHz frequency and 25 μm amplitude (Fig. 2) was used.

During this process, Mylar tape with a one-sided aluminum coating (cathode) is formed into a cylinder shape, and overlapping edges are attached by ultrasonic welding in a straight line with no glue used (so-called “straight adhesion”).

This method allows the production of strong C-shaped straws that can maintain their parameters even after being installed in a stretched position and overpressurized.

For a good operating performance, a homogeneous electric field can be easily achieved. It is necessary to monitor the seam size during straw production and hold it inside the requested area since the seam area is especially responsible for major gas leakage if it takes place - the smaller size of the seam will increase the gas leakage. In contrast, a larger seam will affect the straw tube shape (Fig.

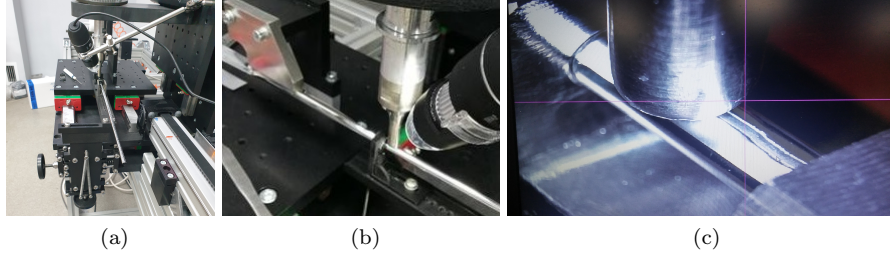


Figure 2: Straw production machine (a); straw welding spot creation (b) and seam forming moment after welding (c)

3). The reason for this gas leakage through the seam is the destruction of the metalized inner layer of the tubes during production. The typical width of the seam for 5-mm 12- μm straw is about 350 μm (Fig. 3a) and the seam thickness is around 22 μm (Fig. 3b, 3c).

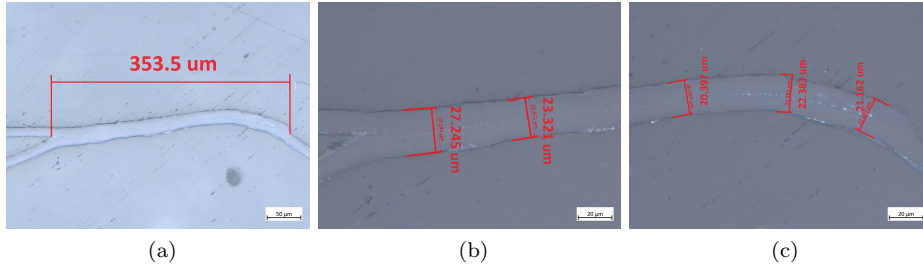


Figure 3: The seam cross-section captured by microscope with magnification of 100x (a); the seam left area (b) and the seam left area (c) with magnification of 400x

A preliminary test of hermetic properties was performed on these 0.6-m-long straws. To perform it, the 3 Bar over-pressure was applied to the tube, and the internal pressure of the straw was continuously monitored for a week with a 1-minute interval (Fig. 4), and the data obtained was fitted using an exponential function. We could estimate the speed of the pressure dropping rate as 0.23 mBar per hour or 4 μBar per minute. Using the Boyle–Mariotte law, we could calculate the gas leakage as (1):

$$\Delta V = V_{str}P_1 - V_{str}P_2 = V_{str}\Delta P \quad (1)$$

Here, V_{str} is the straw tube's internal volume, and we do not take into account volume changes by pressure drop since it is negligible. The ΔP is the rate of pressure dropping.

So, using the equation (1), we can estimate the gas leakage for 0.6-m-long 5-mm with 12- μm -thick wall straw tube at $0.5e^{-4} \text{ cm}^3/\text{min}$ level, or

$0.8e^{-4} \text{ cm}^3/\text{min}$ per 1 meter. The results of the careful and full-scale study of leakage is a subject for another publication.

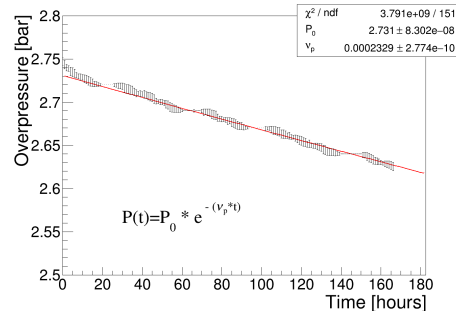


Figure 4: Preliminary test of the gas leakage for the 0.6-m-long 5-mm 12- μm -thick straw

The manufactured straws were scanned for the diameter variations along the straw length to check the production quality. For instance, variations of the straw diameter for different internal over-pressure in the longitudinal direction are presented in Figure 5. Obtained data for each pressure approximated by Gaussian. These variations, once over-pressure delivered into the straw, are inside of $\sigma < 10\mu\text{m}$ (Fig. 5b).

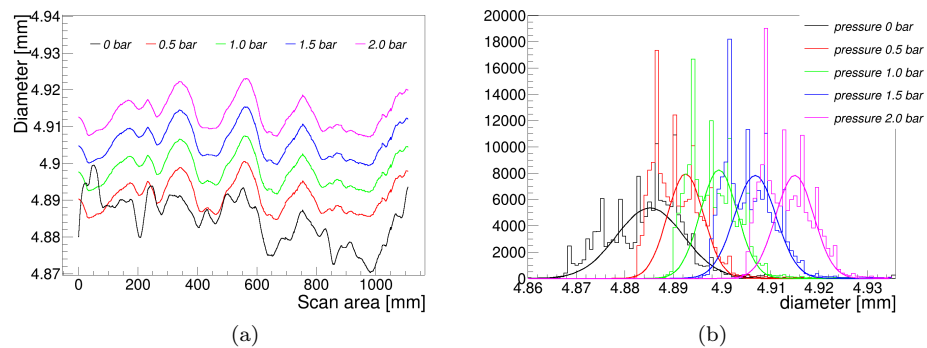


Figure 5: Diameter variations along the straw for different over-pressure. Scanning area - 1100 mm with step of $10 \mu\text{m}$

3. 5-mm-diameter with 12- μm thick wall straw tubes mechanical properties study

About 100 5-mm-diameter 12 μm -thick straw tubes were produced to check production stability. As a next step, the mechanical properties of this type of

straw should be studied. We provided the almost complete set of the mechanical properties study: straw tube elongation VS load; straw tube elongation caused by internal over-pressure, straw tube diameter dependence on load and on internal over-pressure, straw tube bending since over-pressure in a vertical position and sagging caused by gravitation once straw placed horizontally. For instance, very nice measurements for C-type 9.8-mm straw and 18-mm straw with a wall thickness of $36 \mu\text{m}$ and $54 \mu\text{m}$ are done in article [20].

3.1. Setup to provide the measurements

Two unique setups were built to provide the study of the mechanical properties using standard T-slot profiles. Part of it was done using the setup #1, and it was equipped with a 1-X translation stage with attached to it the tension gauge on one end of the straw tube, and the other end was just fixed (Fig. 6a). The rest of the measurements are done on another setup #2 - it was created from scratch to provide more wide tests of the straw tubes (Fig. 6b). This new setup allows us to study the tube's mechanical properties with lengths up to 4.5 m, which can be set on different angles to azimuth from 0 to 90 degrees, etc.

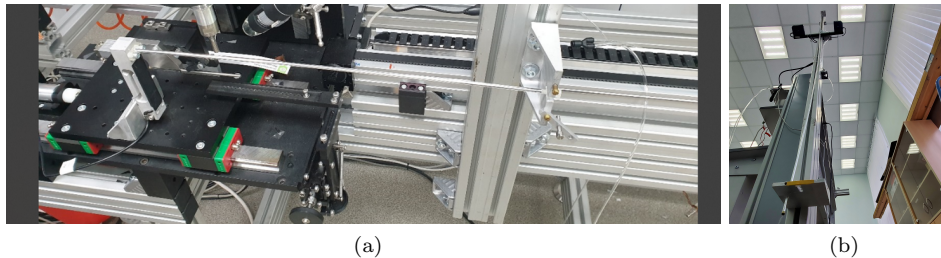


Figure 6: Special setup was built to provide the mechanical properties study: setup #1 (a) and setup #2

To measure the straw diameter variation, sagging, and bending, a Micro-Epsilon "optoCONTROL 2600" laser micrometer was used [21]. The sensor measurement range is based on the width of the laser beam and corresponds to 40 mm with an accuracy of $1 \mu\text{m}$ (Fig. 7). This laser micrometer can operate in different modes, and we only used two of them: "Mode 1" - to measure the position of the edge of "light-dark" in absolute value (Mode 1) and "Mode 2" - to measure the difference of two edges relative values. The first mode allows measuring the straw tube displacement from the initial position, and the second mode allows monitoring of the straw tube diameter during the measurements. This device is installed in the middle of the straw being measured.

The elongation measurements provided on setup #2 are done using the following technique. The narrow laser beam spread into a wide angle using the de-focusing lens. A small paper strip marker is placed on the end of the straw. The straw end with marker was placed in the middle position from the laser source to the screen with a ruler. The light beam was shadowed by a marker,



Figure 7: Micro-Epsilon "optoCONTROL 2600" laser micrometer measures the straw displacement from initial

and we can monitor the variation of the straw length on the screen using a ruler (Fig. 8).

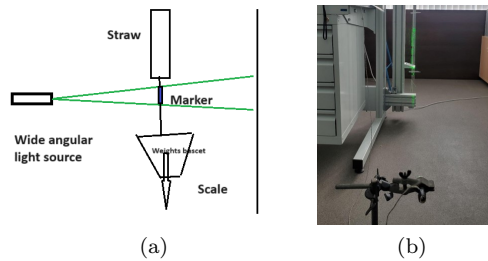


Figure 8: Sketch of the elongation measurements using setup #2 (a) and a view on the setup (b)

3.2. Straw tube elongation study as a function of the external load

The straw tube elongation tests under various load conditions were done for 0.5, 1.0, and 1.34-meter-long tubes under various load conditions.

The elongation test for tubes with 0.5 and 1.0 meter long tubes was done on setup #1 (Fig. 6a) when one end of the straw tube was fixed on the tension gauge and the other end was just constantly fixed. The tension gauge was installed on the 1-X translation stage. The gauge was connected to the computer for remote data acquisition and control. Measurements with these tubes were done with no over-pressure delivered to tubes.

Figure 9 represents the results of these measurements. The graphs were fitted with the linear function to prove that the elongation was within the elastic area according to Hooke's law (2). The stiffness T_p values were found to be equal to 226 g/mm for a 0.5-m-long tube and 123 g/mm for a 1.0-m-long tube.

$$\delta L(f_{load}) = \delta L(0) + \frac{f_{load}}{T_f} \quad (2)$$

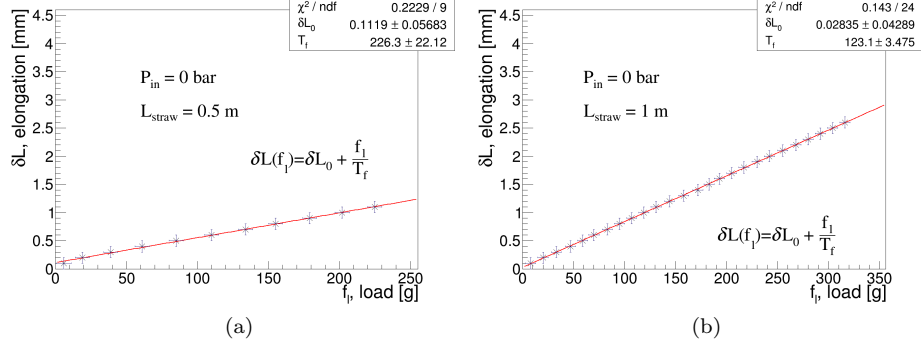


Figure 9: Elongation tests for the 0.5-m and 1.0-m-long 5-mm-diameter straw tubes with $12 \mu\text{m}$ thickness. The results of the elongation for 0.5-meter long tube (a) and for 1-meter long tube (b) with no over-pressure delivered into the tubes.

The elongation test for the 1.34-meter long straw tube was done on setup #2 (Fig. 6b). An over-pressure was delivered into the straw to hold the shape. In this case, the physical weight was used to stress the tube, which was hung vertically. The marker was stuck on the end of the straw tube where the weight basket was installed. A laser widespread light source was used to illuminate the marker, and the position of the marker shadow was monitored on screen with a scale on it located behind the straw tube (Fig. 8). The straw was placed halfway from the light source to the screen with scale. The values of the positions were read out by a camera installed in front of the screen.

The 0.5 and 1.0 bar over-pressure was delivered into the tube to find the difference in stiffness by the external load for different internal pressures. The resulting graph for the 0.5 bar over-pressure case is shown in Figure 10a and for the 1.0 bar - in Figure 10b. Again, according to Hooke's law, both graphs were fitted with linear function (2) for the elastic area. Stiffness values were found to be equal to 80 g/mm for 0.5 bar over-pressure and the same 80 g/mm for 1.0 bar over-pressure. No changes are observed for the stiffness value changing in the internal over-pressure delivered to the straw, and it is expected due to negligible changes in the value of the straw tube cross-section area. So, we can combine the stiffness value for 1.34-m straw with data obtained for 0.5-m and 1-m long straw.

In the case of 1.0 bar over-pressure, the elastic area is limited to a 500-gram load compared to the 0.5 bar over-pressure case, which still is inside the elastic area up to a 700-gram load. Obviously, the limitation of 500 grams for the 1.0 bar case results from the combined stress of the external load and the internal over-pressure.

The stiffness is inversely proportional to the straw tube length in other same

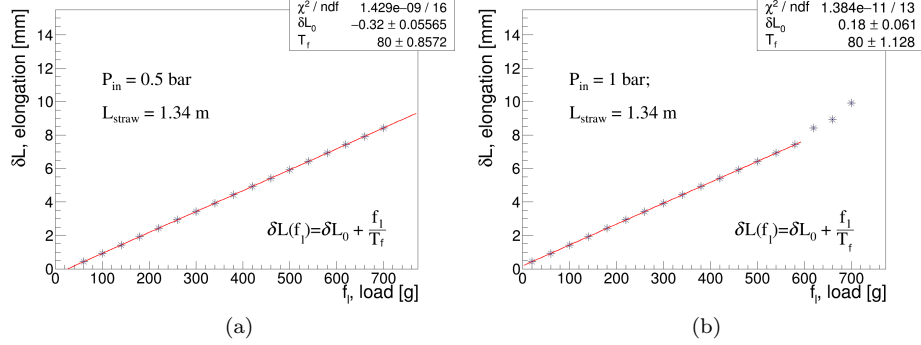


Figure 10: Straw elongation tests for the 1.34 m long 5 mm straw tubes with 12 μm thickness but different over-pressure delivered into the tube. (a) the results of the elongation for 0.5 bar over-pressure case and (b) - for 1 bar over-pressure case

conditions according to well-known equation (3):

$$T_p(L) = \frac{E_m S_{cross}}{L} \quad (3)$$

Here: $T_f(L)$ - is the stiffness, E_m - Young's modulus for mylar, L - length of the straw, S_{cross} - cross-sectional area of the straw tube perpendicular to the load. Please note that the dependencies in the straw cross-section values produced by the load were negligible, and we did not consider them.

In the case of straw tubes, the relation of the thickness of the mylar ($T = 12 \mu\text{m}$) for of the straw tube to its diameter ($D = 5 \text{ mm}$) is small, $D \gg T$ so that the stiffness could be approximated as:

$$T_f(L) = \frac{\pi * E_m * T * D}{L} \quad (4)$$

Figure 11 represents the stiffness dependence by the straw length approximated with a function (4). We got the value for stiffness $T_f = 58.3 \times 10^3 \text{ gr/mm}^2 = 58.3 \text{ kg/mm}^2$. It is equal to 5.7 GPa or $0.83 \times 10^6 \text{ psi}$, and this result is consistent with the 5.24 GPa ($0.76 \times 10^6 \text{ psi}$) obtained for mylar tapes in [22].

3.3. Straw tube elongation by internal pressure

In contrast to the elongation caused by the external load attached to the tube ends, it is also important to know how the elongation acts when the over-pressure is delivered into the straw. So, we measured the elongation as a function of the straw tube internal over-pressure for 0.5 and 1.0-m-long tubes. This study was done on setup #1. Results are represented in Figure 12.

Again, the stiffness coefficient is linearly dependent on the straw length, as was observed for the straw stretch test with external loads described in the previous chapter.

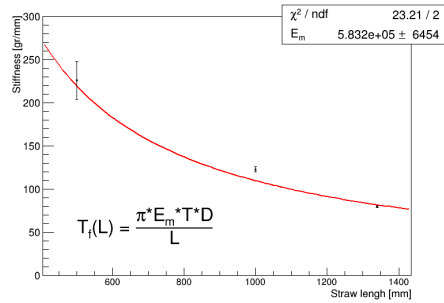


Figure 11: Stiffness coefficient VS length of the straw 5-mm-diameter 12- μm -thick tubes

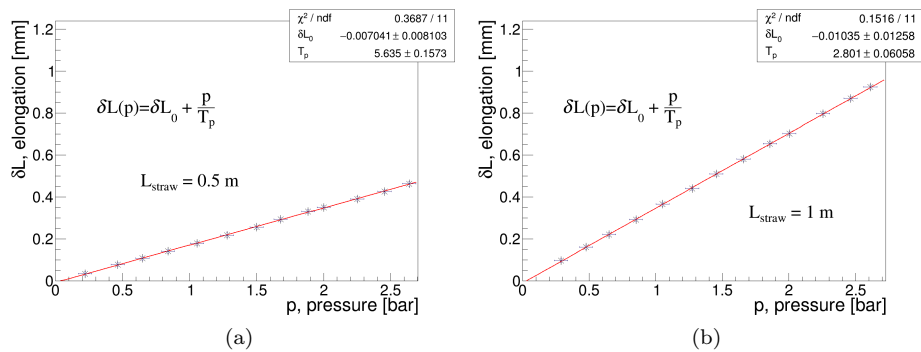


Figure 12: Elongation tests for the 0.5-m and 1.0-m-long 5 mm straw tubes with 12 μm thickness as function of the internal over-pressure. No load attached. The results of the elongation for 0.5-meter long tube (a) and for 1-meter long tube (b)

3.4. Diameter VS load VS over-pressure

Another useful study is to monitor the straw tube diameter dependence on an external load for different internal over-pressures. Results of such test for 1.34-m-long tubes when 0.5 bar and 1.0 bar over-pressure delivered into the straw are represented in Figure 13.

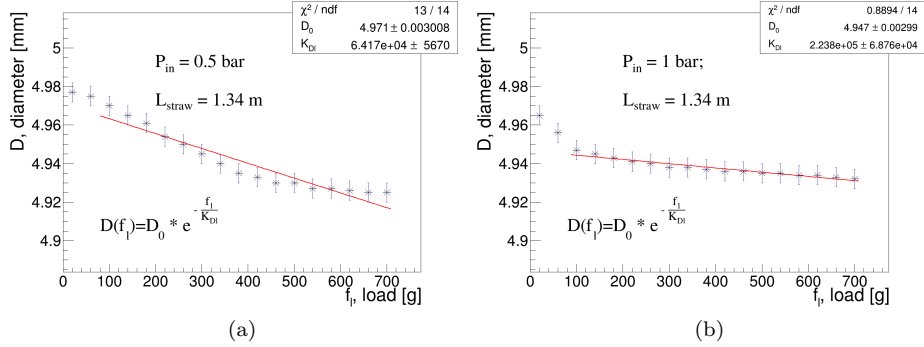


Figure 13: Straw tube diameter dependence on external load for different internal over-pressure: for 0.5 bar (a) and for 1.0 bar (b)

The dependence of the straw diameter along its length on over-pressure was already shown in Figure 5. In addition to that study, in this chapter, Figure 14 presents the dependence of the straw tube diameter on internal over-pressure at the middle of the straw only.

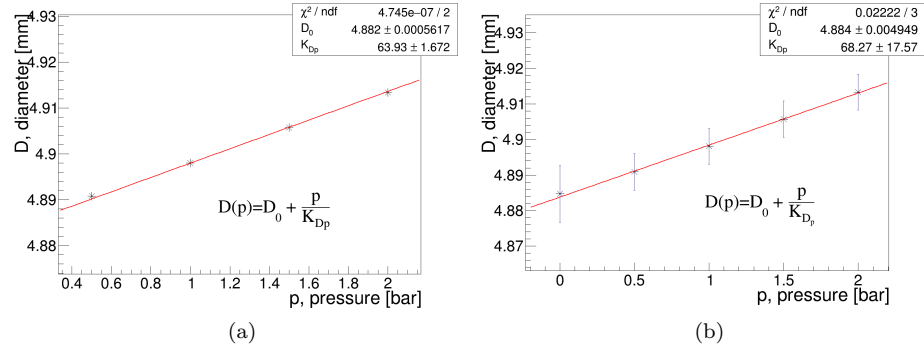


Figure 14: Straw diameter dependence of the over-pressure delivered to the straw: on the center of the 1.34-m-long straw (a) and the mean values of the diameter scanning along the straw (b) according to Figure 5b.

According to these results, the diameter expansion caused by over-pressure is $1/K_{Dp} = 0.016 \text{ mm} = 16 \mu\text{m}$ per 1 bar.

3.5. Straw tube sagging and bending dependencies on external load

The straws are losing their straightness due to bending in vertical installation and due to a combination of bending with sagging (gravitation effects) in horizontal installation. A straw curvature due to these effects exposes the track recovery accuracy. This reason shows the important to study of the straw bending and sagging.

The bending for the 1.34-m-long straw was done for vertical installation, and only the top end was fixed. The result for this measurement is presented in Figure 15a

The sagging for the 1.34-m-long straw was done in horizontal installation, and, again, only one side was fixed, but the other side was loaded. This measurement result is presented in Figure 15b.

Please note that the 0.5 Bar over-pressure was delivered into the straw to keep its shape during these measurements.

The 200 gram is a minimal external load to the straw to hold the straightness of the 1.34-m-long 5-mm-diameter 12 μm -thick straw inside of 200 μm in both cases.

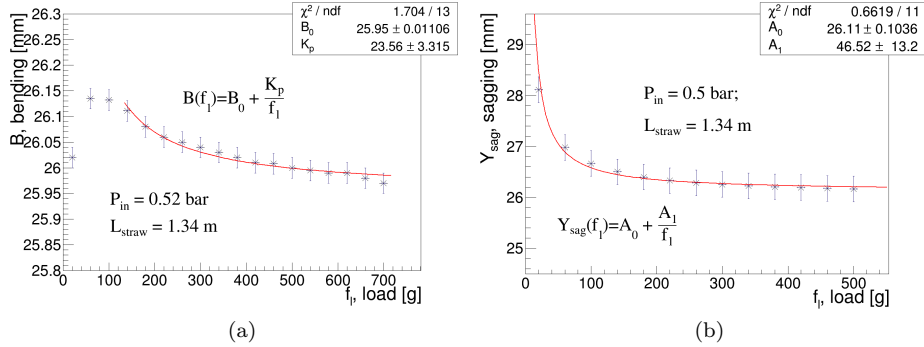


Figure 15: Bending and sagging study for 1.34-m-long 5-mm diameter 12- μm -thick straw

4. Conclusions

The 5-mm-diameter 12- μm wall-thick straw tube production methodology and production station were successfully developed. To prove production stability, more than 1.34-m-long 100 straws were produced.

Two different test setups were created, and different methodologies were used for each setup to carry out the mechanical testing of the tubes. Using this setup, detailed properties studies of the straws were performed: elongation, diameter changes, pressure and load, bending, and sagging.

The elongation study shows that these straws could be loaded with up to 600 grams and remain within the stretching linear area. The Young module was calculated to be about 5.7 GPa.

The straw elongation caused by internal over-pressure proportionally depends on the internal over-pressure. As expected, stiffness for a 0.5-m-long straw was twice higher than for a 1-m-long straw.

As expected, the diameter also depends on the external load on the straw and the internal over-pressure value. It was found that the diameter of the straw expands for 16 μm per 1 bar.

Both bending and sagging studies show that it is necessary to load at least 200 grams to keep the straightness of the 1.34-m-long straw better than 200 μm .

It was experimentally confirmed that straws with this design could hold up to 3 bar over-pressure. This fact allows the straws with a wall of 12 μm to be used for COMET Phase-II with 1 bar over-pressure delivered and operated in a vacuum.

5. Acknowledgments

This work were supported by Shota Rustaveli National Science Foundation of Georgia (SRNSFG), grant number [PHDF-19-3553], by the EU Horizon 2020 Research and Innovation Programme under the EXCELLENT SCIENCE - MSCA, PROBES, GA 101003460 & SRNSFG and by JSPS KAKENHI 21H04482, 16KK0108, and 16H02192

The authors would like to sincerely thank GTU (Tbilisi) and JINR (Dubna) for their strong facility support in performing this study.

We would like to express our gratitude to Guram Tushmalishvili for useful discussion in the field of Material Engineering, and to Iliya Chokheli for supporting this research by providing the design of CAD models and developing them for the test setup.

References

- [1] The COMET Collaboration and Abramishvili, R. and other, COMET Phase-I technical design report, Progress of Theoretical and Experimental Physics 2020 (3) (2020) 033C01. [doi:10.1093/ptep/ptz125](https://doi.org/10.1093/ptep/ptz125).
- [2] E. Hincks, B. Pontecorvo, Search for gamma-radiation in the 2.2-microsecond meson decay process, Phys. Rev. 73 (1947) 257. [doi:10.1103/PhysRev.73.257](https://doi.org/10.1103/PhysRev.73.257).
- [3] R. Barbieri, L. Hall, Signals for supersymmetric unification, Physics Letters B 338 (2) (1994) 212–218. [doi:10.1016/0370-2693\(94\)91368-4](https://doi.org/10.1016/0370-2693(94)91368-4).
- [4] Y. Kuno, Okada, Muon decay and physics beyond the standard model, Rev. Mod. Phys. 73 (2001) 151. [doi:10.1103/RevModPhys.73.151](https://doi.org/10.1103/RevModPhys.73.151).

- [5] S. Mihara, J. Miller, P. Paradisi, G. Piredda, Charged lepton flavor-violation experiments, *Annu. Rev. Nucl. Part. Sci.* 63 (2013) 531. doi:[10.1146/annurev-nucl-102912-144530](https://doi.org/10.1146/annurev-nucl-102912-144530).
- [6] H. Nishiguchi, other, Development of an extremely thin-wall straw tracker operational in vacuum—the comet straw tracker system, *Nuclear Instruments and Methods in Physics Research Section A* 845 (2017) 269–272. doi:[10.1016/j.nima.2016.06.082](https://doi.org/10.1016/j.nima.2016.06.082).
- [7] C. Lu, J. G. Heinrich, K. T. McDonald, R. Burnstein, H. Rubin, D. T. Hackworth, J. W. Bartell, J. Szedon, Proposal to the SSC Laboratory for Research and Development of a Straw-Tube Tracking Subsystem, Tech. rep., SSC-PC-029 (9 1989).
- [8] L. Schieber, *A Straw Tube Design Suitable for Mass Production*, Springer US, Boston, MA, 1990, Ch. Detectors 2, pp. 699–706. doi:[10.1007/978-1-4615-3728-1_64](https://doi.org/10.1007/978-1-4615-3728-1_64).
- [9] V. Bychkov, al., The large size straw drift chambers of the COMPASS experiment, *Nuclear Instruments and Methods in Physics Research Section A: Accelerators, Spectrometers, Detectors and Associated Equipment* 556 (1) (2006) 66–79. doi:[10.1016/j.nima.2005.10.026](https://doi.org/10.1016/j.nima.2005.10.026).
- [10] W. Erni, al, Technical design report for the PANDA (antiproton annihilations at darmstadt) straw tube tracker, *The European Physical Journal A* 49 (2) (2013) 25. doi:[10.1140/epja/i2013-13025-8](https://doi.org/10.1140/epja/i2013-13025-8).
- [11] The ATLAS collaboration, Technical Design Report for the Phase-II Upgrade of the ATLAS TDAQ System, Tech. Rep. 1, CERN (2006). doi:[10.17181/CERN.2LBB.4IAL](https://doi.org/10.17181/CERN.2LBB.4IAL).
- [12] M. Lee, The straw-tube tracker for the mu2e experiment, *Nuclear and Particle Physics Proceedings* 273-275 (2016) 2530–2532, 37th International Conference on High Energy Physics (ICHEP). doi:[10.1016/j.nuclphysbps.2015.09.448](https://doi.org/10.1016/j.nuclphysbps.2015.09.448).
- [13] A. Sergi, Na62 spectrometer: A low mass straw tracker, *Physics Procedia* 37 (2012) 530–534, proceedings of the 2nd International Conference on Technology and Instrumentation in Particle Physics (TIPP 2011). doi:[10.1016/j.phpro.2012.03.713](https://doi.org/10.1016/j.phpro.2012.03.713).
- [14] H. Nishiguchi, et al., Construction on vacuum-compatible straw tracker for COMET Phase-I, *Nucl. Instrum. Meth. A* 958 (2020) 162800. doi:[10.1016/j.nima.2019.162800](https://doi.org/10.1016/j.nima.2019.162800).
- [15] Y. Fukao, et al., Construction Status of the COMET Experimental Facility, in: 12th International Particle Accelerator Conference , 2021, p. 3. doi:[10.18429/JACoW-IPAC2021-TUPAB210](https://doi.org/10.18429/JACoW-IPAC2021-TUPAB210).

- [16] H. Nishiguchi, al, Vacuum-Compatible, Ultra-Thin-Wall Straw Tracker; Detector construction, Thinner straw R&D, and the brand-new graphite-straw development, Nucl. Instrum. Methods Phys. Res. A 1042 (2022) 167373. [doi:10.1016/j.nima.2022.167373](https://doi.org/10.1016/j.nima.2022.167373).
- [17] S. Movchan, Straw tracker prototype for the precise measurement of the very rare decay $k^+ \rightarrow \pi^+ \nu \nu^+$ (na62 experiment at sps cern), Nuclear Instruments and Methods in Physics Research Section A: Accelerators, Spectrometers, Detectors and Associated Equipment 604 (1) (2009) 307–309, pSD8. [doi:10.1016/j.nima.2009.01.223](https://doi.org/10.1016/j.nima.2009.01.223).
- [18] N. Azorskiy, other, A drift chamber with a new type of straws for operation in vacuum, Nuclear Instruments and Methods in Physics Research Section A: Accelerators, Spectrometers, Detectors and Associated Equipment 824 (2016) 569–570, frontier Detectors for Frontier Physics: Proceedings of the 13th Pisa Meeting on Advanced Detectors. [doi:10.1016/j.nima.2015.11.112](https://doi.org/10.1016/j.nima.2015.11.112).
- [19] N. Tsverava, G. Adamov, A. Moiseenko, Nishiguchi, H. Sabirov, Z. Tsamalaidze, Development of ultrathin 12 μm thick straw tubes for the tracking detector of comet experiment, 2019 IEEE Nuclear Science Symposium and Medical Imaging Conference (NSS/MIC) [doi:10.1109/NSS/MIC42101.2019.9060032](https://doi.org/10.1109/NSS/MIC42101.2019.9060032).
- [20] L. Glonti, T. Enik, other, Longitudinal tension and mechanical stability of a pressurized straw tube, Instruments 2 (4). [doi:10.3390/instruments2040027](https://doi.org/10.3390/instruments2040027).
- [21] MICRO-EPSILON Eltrotec GmbH , Göppingen, Germany, Catalog optocontrol optical micrometer, <https://www.micro-epsilon.in/fileadmin/download/products/cat-optoCONTROL-ODC-en.pdf>, (accessed on 03/12/2024).
- [22] H. Becker, Elastic modulus of mylar sheet, Journal of Applied Polymer Science 9 (1965) 911–916. [doi:10.1002/app.1965.070090309](https://doi.org/10.1002/app.1965.070090309).